



Technical note: Temperature dependence of precipitation tail heaviness in the TENAX model

Ella Thomas^{1,2}, Petr Vohnicky¹, Marco Borga¹, Nadav Peleg^{3,4}, and Francesco Marra⁵

¹Department of Land Environment Agriculture and Forestry, University of Padova, Legnaro, Italy

²Institute for Climate and Atmospheric Science, University of Leeds, Leeds, UK

³Institute of Earth Surface Dynamics, University of Lausanne, Lausanne, Switzerland

⁴Expertise Center for Climate Extremes, University of Lausanne, Lausanne, Switzerland

⁵Department of Geosciences, University of Padova, Padua, Italy

Correspondence: Ella Thomas (ee23ert@leeds.ac.uk)

Abstract. Climate change is causing the magnitudes of extreme sub-daily precipitation events to increase. The ability to predict changes to these precipitation extremes is crucial for disaster preparedness. The TENAX model was proposed to predict return levels of sub-daily extreme precipitation under climate change based on the projected temperature shifts. It combines a Weibull distribution with an exponential temperature dependence in the scale parameter, accounting for the Clausius–Clapeyron relation, with an explicit representation of the temperatures during precipitation events. The Weibull distribution’s shape parameter could also have a temperature dependence, which would mean that the tail heaviness changes with temperature. This implies that the rarest events may increase at faster rates. However, implementing this dependence increases the number of parameters to be estimated, affecting the model’s accuracy. Here, we use hourly data from thousands of rain gauges in Germany, Japan, the UK, and the USA to assess the dependence of the Weibull shape parameter on temperature, exploring how it should be implemented in the TENAX model. We find that there is a significant dependence in many stations and that the magnitude and sign of the dependence have regional patterns. In the majority of stations, the sign is negative, implying that rarer events intensify with temperature at a higher rate. However, Monte Carlo simulations show that including this dependence without careful consideration may lead to overestimation of precipitation return levels and increase the model uncertainty. The dependence should therefore be introduced with caution, in the context of surrounding stations.

1 Introduction

Extreme sub-daily precipitation leads to natural hazards such as urban floods, debris flows, and flash flooding. For example, in July 2025, Texas experienced a severe precipitation event, with 130 to 280 mm of rainfall recorded in under 12 h, resulting in flash floods that claimed the lives of over 130 people. (Adams, 2025). On the night of 15 Sept 2022, extreme rainfall, with a peak of 96 mm in one hour, impacted the Misa river in central Italy causing 13 casualties. Record-breaking intermittent heavy rainfall on the southern Japanese island Kyushu caused floods and landslides, resulting in over 60 deaths (Office, 2021). The southern UK town of Boscastle saw a damaging but non-fatal flood in 2004 caused by extreme localised rainfall. In one location, 86 mm of rain was recorded in one hour (Burt, 2005). Extreme events such as these are often discussed in relation to



anthropogenic climate change (Pall et al., 2011; Faranda et al., 2025; Kawase et al., 2020). It is difficult to attribute individual extreme events directly to climate change, but they are rarely seen in the historical record and are expected to increase in frequency and magnitude in the future (Fowler et al., 2021; Ebers et al., 2024; O’Gorman, 2015).

The intensification of extreme short-duration precipitation with temperature is assumed to follow the increase of atmospheric water vapour, which follows the Clausius-Clapeyron relationship, pointing to a potential intensification of $7\% \text{ }^{\circ}\text{C}^{-1}$ in ideal atmospheric conditions (Trenberth et al., 2003). However, observational studies have found that extreme precipitation may scale with temperature differently than this theoretical value in various parts of the world (Guerreiro et al., 2024; Ali et al., 2021). Ali et al. (2021) found that scaling rates over the ocean are larger than over the land, and scaling rates are especially low or negative in tropical and dry regions. Dynamic factors, such as orography, changes in the location of the intertropical convergence zone, and large-scale moisture transport mechanisms, also impact the scaling rates (Pfahl et al., 2017).

Few methods are currently available that incorporate these rainfall-temperature scaling rates into predictions of rare precipitation return levels (e.g., Ebers et al., 2024). Among these is the TEMperature-dependent Non-Asymptotic model for eXtreme return levels (TENAX) proposed by Marra et al. (2024), which requires only rainfall and temperature data and has minimal parameters. Assuming that thermodynamics is the main factor enhancing rainfall convection at short-duration (Fowler et al., 2021), near-surface air temperature can be used as the primary covariate that explains intensification of rainfall extremes (Lenderink and van Meijgaard, 2008). Hence, assuming that the relation between temperature and precipitation does not change with climate change (i.e., it is a physical invariant, Held and Soden, 2006), changes in return levels of extreme precipitation can be predicted based on the temperatures at which precipitation events occur, which can be defined according to the predictions of different climate change scenarios. So far, this framework has been tested in the Alps (Peleg et al., 2025), Switzerland (Marra et al., 2024; Peleg et al., 2024), and Germany (Laux et al., 2025). Its predictions were validated using hindcasts, which showed good performance in the majority of the stations.

Practically, TENAX relates the exceedance probability of high magnitudes of precipitation to the temperatures during precipitation using a non-stationary Weibull distribution (as motivated by Wilson and Toumi, 2005). This distribution is described by a scale parameter and by a shape parameter that determines the tail heaviness of the distribution, that is, how much larger extremes are with respect to the average. So far, the temperature dependence was only included in the scale parameter using an exponential dependence that approximates the Clausius-Clapeyron equation. However, observational studies have suggested that the scaling rate may vary between different percentiles of extremes, which would imply a temperature dependence in the shape parameter of the distribution (Lenderink and van Meijgaard, 2008; Hardwick Jones et al., 2010). For example, Hardwick Jones et al. (2010) found that scaling increased from approximately $5\% \text{ }^{\circ}\text{C}^{-1}$ at the 75th percentile to $7.5\% \text{ }^{\circ}\text{C}^{-1}$ at the 99th percentile. The implications of this dependence are substantial, as it affects the rate of increase with temperature of the rarest and most extreme events. Marra et al. (2024) and Peleg et al. (2025) tested a linear dependence on temperature in the shape parameter and found that there was no statistically significant dependence at the stations in the Alps. Conversely, Andria et al. (2025) used a similar framework in the United States to find that an exponential relation well approximates the temperature dependence of the shape parameter. These contrasting results lead to the question of whether a dependence of the shape parameter on temperature should be included when using this type of model. If there is a dependence, there are three



main options for dealing with the parameter that defines the dependence: it can be allowed to vary freely at a particular station, it can be set to a reasonable value based on prior knowledge of the climatology of the region, or it can be neglected (although it exists).

Here, we investigate how the temperature dependence can be estimated from observed records without introducing large errors and uncertainty. Specifically, we answer the following questions: (i) does the shape parameter exhibit a significant dependence on temperature in different regions of the world? If there is a dependence, how does its direction and magnitude vary in space?; (ii) how much of the observed variation in such dependence can be attributed to spatial variability rather than sampling uncertainty?; (iii) does including this dependence influence the time-invariance assumption behind these approaches?; and (iv) does this dependence affect the estimates of return levels? How is this affected by the length of the data record? We conclude by giving some practical recommendations for when and if a dependence of the shape parameter of the Weibull magnitude model should be included in the TENAX-like frameworks.

2 The TENAX model

A full description of TENAX can be found in Marra et al. (2024). Here, we summarise the basics necessary for this paper. First, independent precipitation events are identified. These are defined as the peak precipitation intensities observed over the duration of interest, in our case, 1 h, during an independent storm. To ensure independence, storms are required to be separated by a minimum of 24 dry hours. The temperature value T assigned to an event is the temperature averaged in the 24 h preceding the event. TENAX includes a temperature model $g(T)$, which quantifies the probability of having a precipitation event at a given temperature, and a magnitude model $W(x; T)$, which quantifies the exceedance probability of heavy precipitation magnitudes for events at a given temperature.

For the temperature model, we use a generalised normal distribution with shape parameter $\beta = 4$:

$$g(T) = \frac{2}{\sigma \Gamma\left(\frac{1}{\beta}\right)} \exp \left[- \left(\frac{T - \mu}{\sigma} \right)^\beta \right]. \quad (1)$$

The location parameter μ and the scale parameter σ are estimated using the maximum likelihood method.

TENAX's magnitude model is a non-stationary Weibull distribution, with temperature as the covariate. A Weibull distribution was chosen because this should approximate the tail of heavy precipitation based on atmospheric physics arguments (Wilson and Toumi, 2005). It is given by:

$$W(x; T) = 1 - \exp \left(- \left[\frac{x}{\lambda(T)} \right]^{\kappa(T)} \right), \quad (2)$$

where $\lambda(T)$ is the scale parameter and $\kappa(T)$ is the shape parameter. Since extreme precipitation is expected to scale exponentially with temperature following the Clausius-Clapeyron relationship (Fowler et al., 2021), an exponential dependence on temperature T is used in the scale parameter: $\lambda(T) = \lambda_0 e^{aT}$. The shape parameter affects the tail-heaviness of the Weibull distribution, and previous observational studies have suggested that this might also have a dependence on temperature (Lenderink



and van Meijgaard, 2008; Hardwick Jones et al., 2010). We investigate both a linear and exponential dependence in the shape parameter, namely $\kappa(T) = \kappa_0 + bT$ or $\kappa(T) = \kappa_0 e^{b_{\text{exp}} T}$. The parameters in the magnitude model are estimated by left-censoring the values below the 90th percentile of the events, meaning that the values below this threshold are retained for the estimation and treated as non-exceedances (see Marra et al., 2020), using a maximum likelihood estimator.

The combination of the magnitude model $W(x; T)$ and the temperature model $g(T)$ using the total probability theorem gives the cumulative distribution function of the event magnitudes:

$$F(x) = \int_0^{\infty} W(x; T) \cdot g(T) dT. \quad (3)$$

The cumulative distribution function of the annual maxima emerging from independent samples is then given by $G(x) = F(x)^n$, where n is the average number of events per year (Marra et al., 2020). Since the integral in Eq. 3 doesn't have a practical closed-form solution, a Monte Carlo approximation with $N = 2 \cdot 10^5$ iterations is used. Hence,

$$G_{\text{TENAX}}(x) = \left(\frac{1}{N} \sum_{i=1}^N W(x; T_i) \right)^n, \quad (4)$$

where T_i are temperatures sampled from $g(T)$. Return levels are calculated by inverting equation 4 numerically.

3 Precipitation and temperature data

Hourly precipitation data were taken from the global sub-daily rainfall (GSDR) dataset (Lewis et al., 2019). The data lengths vary greatly. For our initial spatial analysis (see Section 4), we used stations with at least 10 years of complete data, where a complete year is defined as one with less than 10% missing data. When investigating hindcasts (see next), we only used stations with at least 20 complete years. We focused our analysis on the four countries with the highest number of stations meeting the 10-year completeness criterion: the UK (913 stations), the USA (1365), Germany (696), and Japan (1207).

Hourly temperature data were obtained from the ERA5-land reanalysis dataset (Muñoz-Sabater et al., 2021). The ERA5-land grid cell closest to the coordinates of each station was chosen. The majority (94%) of stations had temperature data within the same grid cell. The average distance between the coordinates of a station and the ERA5-land cell was 4 km. If there were no grid cells with data within 0.5° distance of a station, the station was not used in our analysis.

4 Analysis

First, we calculated the parameters of the TENAX model at each station with more than 10 years of complete data using maximum likelihood estimation and a likelihood ratio test to check whether b was significantly different from 0 at the 5% significance level. The parameters were estimated three times: for both the linear and exponential formulation of the model ("free b ") and for the case when b was set to zero (" $b = 0$ ").

The parameters of the TENAX model are estimated from a finite set of events, and as such, there is a stochastic uncertainty caused by the limited sample size. To investigate the stochastic uncertainty and its relation to b , we performed Monte Carlo



simulations. For each station in a country, we stochastically calculated the parameters five times the number of events observed at each station. We simulated the events using the observed parameter's average over the entire country, and calculated the parameters including and excluding b . The distribution of these parameters represents the expected stochastic spread due to sampling uncertainty. For a summary of the values used to produce the Monte Carlo simulations, see Supplementary Table S1. To directly compare the spread of the generated and observed parameters, we calculated the ratio of the interquartile ranges.

As per TENAX's assumptions, the parameters of the magnitude model are required to be time-invariant. We investigated the effects of b on this time invariance in a hindcast setup. We split the time series at each station in half and computed the parameters of the magnitude model in each half separately. To compare each parameter between the two time periods, we calculated the root mean square difference and the Pearson's correlation coefficient in space. We also compare the magnitude model as a whole by using a likelihood ratio test to see if the model is significantly different between the two periods.

Finally, we used Monte Carlo simulations to understand the impact of b on the accuracy of the estimated return levels. We did this by choosing three representative values of b : -0.015 , 0 , and 0.015 $^{\circ}\text{C}^{-1}$, and typical values for the other parameters: $a = 0.07$ $^{\circ}\text{C}^{-1}$, $\lambda_0 = 1$ mm h^{-1} , $\kappa_0 = 1.1$, $\mu = 10$ $^{\circ}\text{C}$, and $\sigma = 13$ $^{\circ}\text{C}$. We created synthetic data sets of precipitation and temperature events, assuming 80 events per year for 10-, 20-, and 30-year record lengths. From the synthetic data, we estimated the parameters with three different techniques: letting b be fitted ("free"), and setting b to the value used to generate ("set"), therefore mimicking a situation in which b is known (for example, in virtue of the local climatology), and setting $b = 0$. We then compared the return levels resulting from these different estimates with the "true" return levels obtained from the original generating parameters. This is repeated 1000 times to get a range of the possible return levels a single distribution can generate using different techniques. We calculated the "bias in return levels" as the ratio of the recalculated return levels to the expected return levels.

5 Results

5.1 Significant dependence on temperature in the tail heaviness

The significant dependence of the shape parameter on temperature across different regions of the world is presented in Figure 1 for the linear formulation of b . Results for the exponential formulation, which show similar patterns, are provided in Supplementary Figure S1 and are not discussed. The b parameter is significantly different from zero (p.v. of 5%) in 36% of stations in Japan, 44% of stations in the UK, 14% of stations in Germany, and 28% of stations in the USA. The majority of significant b values, as well as their average value, are negative in all regions, meaning that the temperature-precipitation scaling of rarer extremes tends to be higher than that of milder extremes.

In Germany, the locations of stations with significant b are randomly distributed, as is the magnitude of b (Figure 1c). Despite the random distribution of b in Germany, a one-sample Student's t-test shows that the average value of b is significantly different from zero at 1% significance level, pointing to an average value (standard deviation) of -0.012 $^{\circ}\text{C}^{-1}$ (0.017 $^{\circ}\text{C}^{-1}$) for the country. In contrast, Japan, the USA, and the UK show a spatial pattern in the size and magnitude of b . In Japan (Figure 1a), significant negative values are clustered mainly in the southern half of the country, along the central ridge, and in the

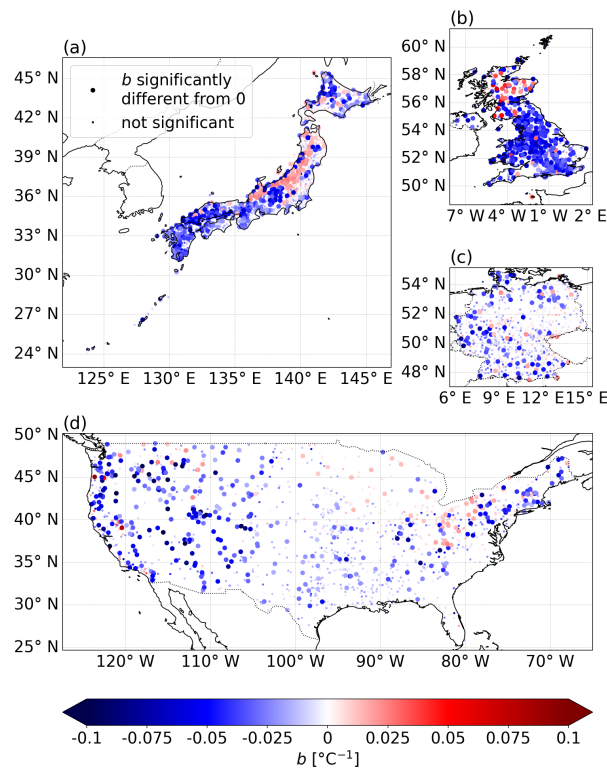


Figure 1. The values of the temperature coefficient in the shape parameter b calculated at stations in (a) Japan, (b) the UK, (c) Germany, and (d) the USA. Larger points are the stations where b is significantly different from zero at 5% significance.

northernmost part of the country. Significant positive b values are clustered in north-central Japan. The average value of b throughout all Japan is $-0.013\text{ }^{\circ}\text{C}^{-1}$ ($0.022\text{ }^{\circ}\text{C}^{-1}$). In the central and south USA (Figure 1d), between approximately 105°W and 95°W , b in the majority of stations (85%) is not significantly different from zero. However, further west of 105°W , only 51% of the b values are not significant. Of the significant values in that region, 94% are negative. In the north-west, there is a mixture of positive and negative significant b values. Focussing on the region east of 95°W and north of 38°N , we find that 74% of stations here have non-significant b . Of those that are significant, 62.5% are negative, a lower value than in other regions. The average of all b values in the USA is $-0.015\text{ }^{\circ}\text{C}^{-1}$ ($0.024\text{ }^{\circ}\text{C}^{-1}$). In the UK (Figure 1b), positive values of b are more likely to be found north of 55°N . However, the average in this region is still negative: $-0.012\text{ }^{\circ}\text{C}^{-1}$ ($0.032\text{ }^{\circ}\text{C}^{-1}$). South of here, the majority of values are negative, with an average value of $-0.027\text{ }^{\circ}\text{C}^{-1}$ ($0.022\text{ }^{\circ}\text{C}^{-1}$). The average value of b in the entire UK is $-0.024\text{ }^{\circ}\text{C}^{-1}$ ($0.025\text{ }^{\circ}\text{C}^{-1}$). Overall, b is significantly different from zero in many locations, and exhibits some regional dependence. It seems to be linked to a range of factors, including latitude, elevation, climatic conditions, and prevalent synoptic forcing.

5.2 Disentangling stochastic uncertainty and spatial variability

Violin plots of the parameter estimates for both the observed and Monte Carlo generated parameters are presented in Figure 2 for the linear b formulation (and in Supplementary Figure S2 for the exponential formulation). All four regions and all parameters have a smaller spread in the generated parameters than in the observed ones, so not all the variation in the observations can be explained by stochastic uncertainty alone. Table 1 shows the ratios of the interquartile range between the generated and observed values (Supplementary Table S2 presents the ratios for the exponential case). A larger value means a greater proportion of the spread can be explained stochastically. For b , the country with the most spatial variation is Japan. Germany has the least spatial variation, as expected from the number of significant values discussed in section 5.1. The other parameters, λ_0 , a , and κ_0 , also present a larger range of values than expected from stochastic variability alone in all the regions. In general, there is not much consistency between the countries in which the parameter has the largest amount of variation.

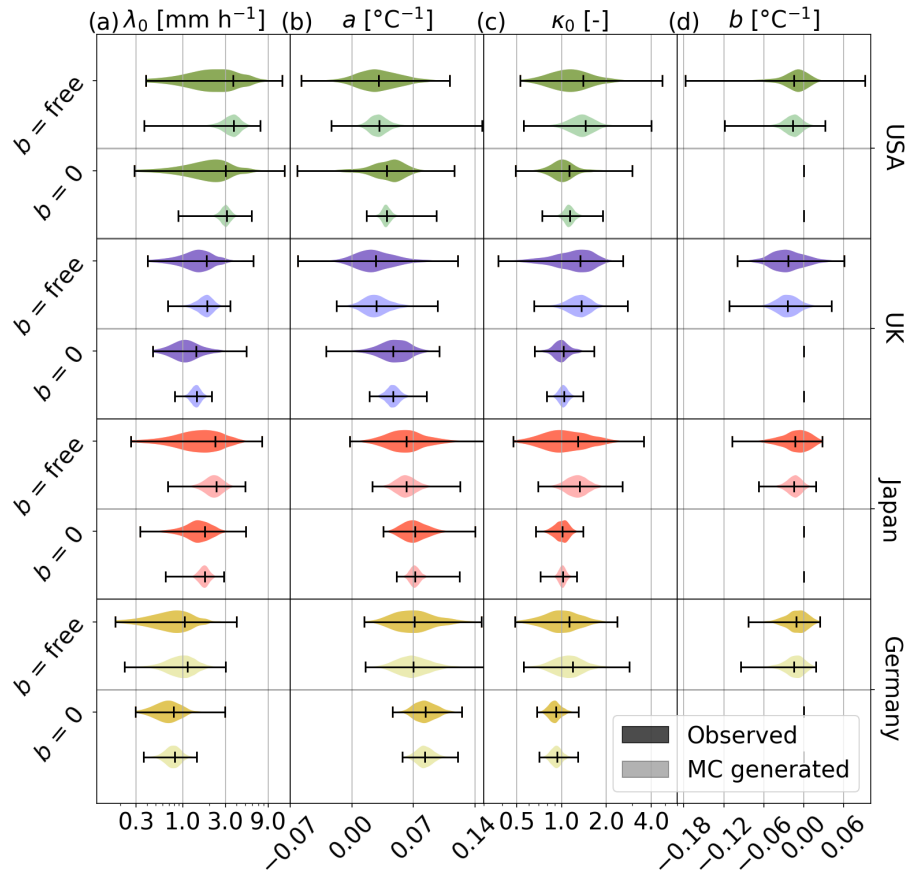


Figure 2. Distribution of parameters of the magnitude model in the USA (green), UK (blue), Japan (red), and Germany (yellow). The darker plots are the observed values, and the lighter plots are the Monte Carlo generated values. In each country, the upper two plots are the parameters when b is fitted freely, and the lower two plots are the parameters when $b = 0$.



Table 1. The ratio of the interquartile range of the generated parameters to the interquartile range of the observed parameters in each country.

Parameter	$b = \text{free}$				$b = 0$			
	Germany	Japan	UK	US	Germany	Japan	UK	US
λ_0	0.86	0.48	0.53	0.38	0.65	0.40	0.34	0.28
a	0.79	0.53	0.62	0.42	0.74	0.39	0.41	0.26
κ_0	0.86	0.48	0.63	0.61	0.88	0.50	0.60	0.45
b	0.90	0.52	0.65	0.71	-	-	-	-

Note that there are 5 times as many simulated parameters as observed parameters. This does not affect the interquartile ranges, but does increase the likelihood of outliers. Hence, some of the simulated violin plots in Figure 2 appear to have a greater range than the observed ones. The increase in outliers shows that the number of events at a station affects the uncertainty in estimating the parameters. For experiments run without these 5 repeats, see Supplementary Figures S3 and S4 and Supplementary Tables S3 and S4.

Comparing the free b with the b set to zero scenarios (Figure 2), we spot a reduction in the spread in the values both in the observations and in the Monte Carlo generated samples. When $b = 0$, the parameter a is the scaling rate between extreme hourly precipitation and temperature, expected to be close to $0.07 \text{ }^\circ\text{C}^{-1}$. On average, this is approximately the case for Japan and Germany. When b is introduced (i.e., non-zero), the average values of a shift to lower values (which means weaker scaling rates) to accommodate the negative b (which means stronger scaling at rarer probabilities). For example, in Japan, the average value of a is reduced from $0.072 \text{ }^\circ\text{C}^{-1}$ in the case of b equal to zero to $0.062 \text{ }^\circ\text{C}^{-1}$ when b is free.

When $b = 0$, the ratio is reduced for almost all parameters and locations (Table 1). This means that a larger amount of the variability is due to genuine variation, rather than stochasticity. This is because including the additional parameter b inflates the parameter estimation uncertainty, while the spatial variability changes less. Overall, the distribution of b in Germany can largely be attributed to stochasticity, while in other countries there is a large amount of spatial variability. Including b in the model, however, largely increases the stochastic spread of the other parameters.

5.3 Time-invariance of the magnitude model

Figure 3 presents scatter plots of the parameters of the magnitude model $W(x; T)$ in hindcast mode, i.e., by splitting the data for each station into two periods. In general, all parameters follow the one-to-one line with some outliers. When $b = 0$, all the parameters follow the line more closely and the correlations increase, especially for the parameter κ_0 , which is strongly influenced by b .

The time invariance of the magnitude model as a whole can be assessed by testing if the model produces significantly different results when applied to the two periods separately compared with the entire time series. Figure 4 shows which stations have significantly different magnitude models at 5% significance when b is included or set to zero. In all countries, the majority of stations do not display significant differences in both cases (66% to 86% of stations). The USA has the largest

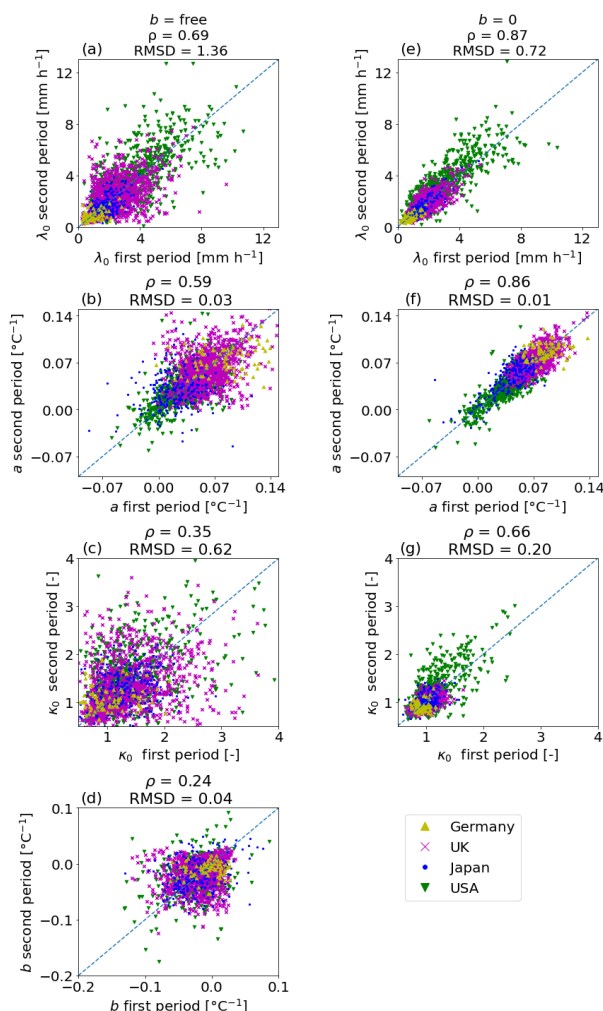


Figure 3. Scatter plots of the parameters in the magnitude model when the time series is split in half (hindcast mode). Left column (a to d) is for $b = \text{free}$ and right column (e to g) is for $b = 0$. Colours represent the country the station is in, and the one-to-one line is plotted in blue dashes.

proportion of stations that have significantly different magnitude models. Of these, 75% are significant regardless of whether b is included. Slightly more stations (4.4%) are significant when b is included than not (4.2%). Germany is also inconclusive, with the same number of stations being significant in one case as in the other. However, in the UK and Japan, the number of stations that have significant differences when b is included but not when $b = 0$ was over double the amount in the opposite case. It is therefore difficult to understand the extent to which including b affects the hindcast significance. However, the scatter plots and correlation coefficients show that freely estimating b from the observations largely increases the variability in the other parameters between the two time periods, as a consequence of the increased stochastic uncertainty.

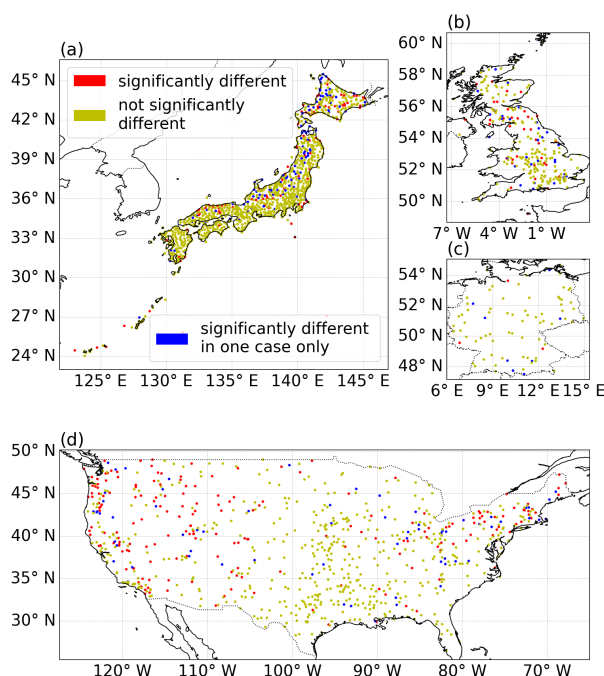


Figure 4. Maps showing where differences in the magnitude models are significant (red) or not significant (yellow), regardless of whether b is fixed to zero or allowed to vary freely, as well as regions where the significance depends on the treatment of b .

205 Using the exponential instead of the linear dependence in the shape parameter produces similar correlations for λ_0 , a , and b_{exp} but reduces the correlation in κ_0 by a substantial amount (Supplementary Figure S5). This is in part due to the presence of large outliers. In fact, the exponential dependence has a dampening effect on the potential magnitude of precipitation. It appears that in some cases, this causes the parameters to over-compensate in the model, leading to unreasonable values.

5.4 Impact on return level estimates

210 To assess the potential influence of b on the estimates of rainfall return levels, we present the ratio between return levels derived using the model in different setups and the “true” return levels obtained from the known synthetic parameters (Figure 5). Note that these are completely synthetic. We chose λ_0 , a , κ_0 , b , μ , σ and n to be representative of the typical observed values. When b is negative (Figure 5a), the variation in return levels is the highest. Allowing b to be fitted and setting b to the known value produce results that are, on average and as expected, the closest to the actual return level, while setting b to zero underestimates
 215 the return levels, especially at higher return periods. When shorter record lengths are used to estimate b , however, the error increases vastly, especially for higher return periods, and fitting b results in unrealistically large return levels. The mean values of the estimated return levels when b is fitted are larger than the median, implying positive skew. The linear and exponential treatments of b have similar patterns, but the variation in the exponential distributions is smaller, and there are fewer large outliers leading to overestimation of return levels (Supplementary Figure S6).

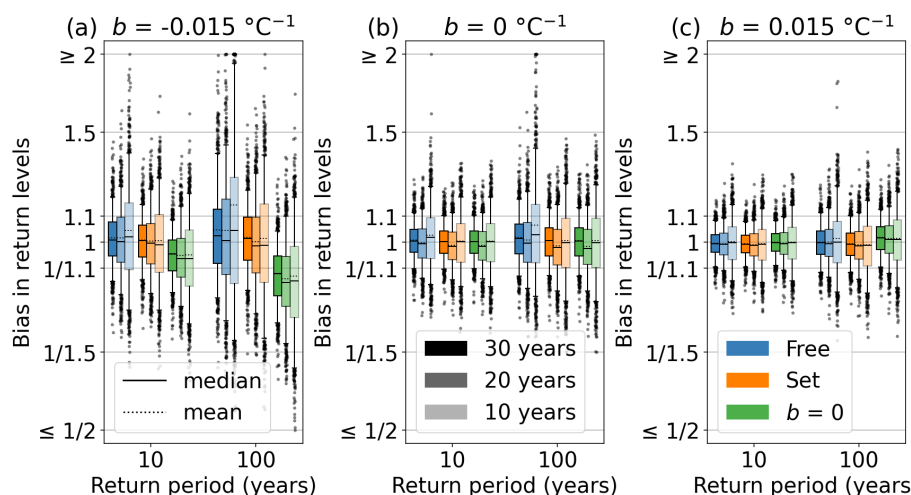


Figure 5. The bias in synthetic return levels for different values of b . The whiskers of the box plots are the 5-95th percentiles. Bar colours represent b setup as allowed to vary (blue), set to its actual value (orange), or set to 0 (green). Bars' opacity represents the record length generated by the model (30-, 20-, and 10-year).

220 When generating a scenario in which b is zero (Figure 5b), letting b vary in the model (blue) leads to overestimation of return levels. This is more pronounced at higher return periods and with shorter data lengths. In this case, “Set” and “ $b=0$ ” are equivalent. All methods produce an average value that is close to the expected return level, but fitting b produces more outliers, especially ones that overestimate the return levels.

225 When b is positive (Figure 5c), the variation in estimated return levels is smaller, likely because the return levels themselves are lower. Still, letting b be free results in larger outliers than the other methods, especially with shorter record lengths and at high return periods. Using $b=0$ in this case leads to overestimation of return levels, but not to the same extent as the underestimation for negative b . Since the observed values of b are more commonly negative than positive, the main concern should be with the potential of underestimation if $b=0$ than this overestimation.

6 Discussion

230 We find that the shape parameter in TENAX shows a statistically significant dependence on temperature in many locations. The typical value of this dependence (negative b parameter, Fig. 1) indicates that the temperature-precipitation scaling of rarer extremes tends to be higher than that of milder extremes. Including this negative b will lead to larger estimated return levels, especially at longer return periods (Fig. 5). It would be beneficial for future work to further explore in detail the physical reasons for the spatial variability of the b parameter. It could be linked to, for example, orography, elevation, or large-scale dynamical drivers. A Bayesian framework for calculating b , and the parameters of TENAX more generally, would also help to
 235 understand and reduce uncertainty.



Andria et al. (2025) suggest that this dependence should be exponential. We find that the difference between exponential and linear dependence is small, although the exponential dependence seems to cause larger uncertainties in the other parameters of the model. In this concern, it should be noted that Andria et al. (2025) use a different statistical setup, in which temperature bins are identified and several parameter sets are estimated without resorting to left censoring. The dependence of the shape parameter on temperature is then assessed ex post. Hardwick Jones et al. (2010) found that the observed scaling in east Australia increased by about 50% between the 75th and the 99th percentile. For the average values of the parameters in Japan, we find an increase of about 20% between these two percentiles. In the USA, the scaling rates are smaller, but with the average values, we also find an increase of 50% between the 75th and 99th percentile.

We note that some stations in the GSDR dataset had a change in the sampling resolution of precipitation during the observation period. For example, the resolution of some records changed from 2.54 mm h^{-1} to 0.254 mm h^{-1} . This may affect the calculations of the parameters and the hindcasts. We re-run our analyses excluding all these stations, but no differences in the results could be noticed. Removing stations with less than 20 years of available observations from the hindcasts was more effective in reducing the presence of extreme outliers. We conclude that the data length is more important to the quality of the results than consistency in resolution.

To match temperature values to precipitation, we used a reanalysis dataset. This may not align with the actual near-surface air temperature that one would measure using ground observations, especially on the scale of individual stations. Mistry et al. (2022) found that there was a high correlation between the observed daily temperatures at stations and the temperatures produced by ERA5-land, especially in the countries we investigate. Although Sheridan et al. (2020) found that ERA5 was better than ERA5-land at representing extreme heat events, we chose to use ERA5-land for its finer resolution. Other products, such as regional ones, may give more accurate temperatures, but would not allow us to compare study areas across the globe. In any case, temperatures are averaged over the 24 hours preceding each event, limiting the potential impact of misrepresenting the location of small-scale weather events in ERA5-land. When producing the stochastic simulations of the parameters, we used the temperature model given in Eq. 1. In some locations, this may not give an accurate range of temperature values. Given infinite events, the magnitude model and temperature model are independent, so the temperature model used would not affect the parameters of the magnitude model. However, within a finite sample, the limited temperature values may affect the magnitude model.

6.1 Practical recommendations

While the spatial variability observed in b cannot be attributed solely to stochastic uncertainty, the stochastic component is of the same order of magnitude as the spatial variability (Fig. 2). This contrasting behaviour brings the fundamental question of whether the dependence should be allowed in practical applications.

When producing models for extreme rainfall with temperature as a covariate, we recommend checking if there is a temperature dependence in the shape parameter and investigating its behaviour when using an exponential and linear dependence. Excluding b will often lead to underestimation of the return levels, especially at longer return periods. In contrast, leaving b to be freely estimated from the (usually limited) observations is associated with large uncertainty, leading to noisy estimates



and, often, to unrealistic estimates of the return levels. Developing some prior knowledge about b in a region of interest can largely improve our estimates. In particular, setting b to a chosen, realistic non-zero value seems a good compromise. If there are enough stations with sufficiently long measurements in a region of interest, b can be set to the average calculated value of b in the region. If this is not possible, setting $b = 0$ remains the recommended option, with the awareness that larger return levels might be underestimated.

7 Conclusions

We investigated the dependence of heavy hourly precipitation tail heaviness on temperature using the framework provided by the TENAX model (Marra et al., 2024) for multiple stations worldwide. We found that in many of the stations the shape parameter of the distribution exhibits a significant dependence on temperature ($b \neq 0$). The sign and size of this dependence present a spatial pattern and appear to be linked to latitude, elevation, climatic conditions, and large-scale drivers. Future work could investigate these influences specifically. Monte Carlo simulations show that, aside from Germany, the variation within the countries investigated is not attributable to stochastic uncertainty alone. Including b in the magnitude model increases the variability in the other parameters of the magnitude model, but does not make a large difference to whether the magnitude model is invariant in time when performing hindcasts. Calculating b from data at a single station may lead to a large overestimation of return levels, especially for stations with shorter record lengths. Using an exponential dependence rather than a linear one somewhat mitigates against this, but yields larger uncertainties in the remaining model parameters.

With these conclusions in mind, we recommend the following. If only short record lengths are available (between 10 and 20 years), b should not be estimated from the individual stations alone, since the uncertainty introduced may severely bias the estimation of the return levels and of the other parameters in the magnitude model, leading to inconsistent projections. At the same time, b should not be neglected completely, since it is certainly non-zero in many regions, and its exclusion leads to an underestimation of return levels. Having prior knowledge about this dependence would largely improve the estimates. In ideal conditions, b should be estimated in the context of surrounding stations, with care to ensure the values are physically reasonable. Setting b to a reasonable, well-supported, non-zero value, such as the average value within an adequately identified region, would be a viable option to reduce these uncertainties while retaining the physical meaning of this parameter. When no prior information on b is available, setting it to zero remains the recommended option.

Code availability. The Python version of the TENAX model used in this study, *pyTENAX* (Vohnicky et al., 2025), is freely available at <https://github.com/PetrVey/pyTENAX>. The code to reproduce results in this paper will be uploaded upon in their final version upon acceptance. The MATLAB version, used in Marra et al. (2024), is available at <https://zenodo.org/records/15291014> (Marra and Peleg, 2025).

Data availability. The global sub-daily rainfall (GSDR) dataset is available at <https://zenodo.org/records/8369987>, and the ERA5-land reanalysis dataset can be downloaded from <https://cds.climate.copernicus.eu/datasets/reanalysis-era5-land>.



Author contributions. Conceptualization: ET, FM, NP, MB; software development: ET, PV, FM; data preparation: ET; formal analyses: ET; funding acquisition: MB, FM; paper writing – original draft: ET; paper writing – review and editing: ET, FM, PV, NP, MB.

Competing interests. At least one of the (co-)authors is a member of the editorial board of Hydrology and Earth System Sciences.

305 *Acknowledgements.* This study was supported by the Department of Geosciences of the University of Padova (TENAX project) as part
of “The Geosciences for Sustainable Development” project (Budget Ministero dell’Università e della Ricerca–Dipartimenti di Eccellenza
2023–2027 C93C23002690001) and by the RETURN Extended Partnership which received funding from the European Union Next-GenerationEU
(National Recovery and Resilience Plan – NRRP, Mission 4, Component 2, Investment 1.3 – D.D. 1243 2/8/2022, PE0000005). NP was sup-
ported by the Swiss National Science Foundation (SNSF Grant number: 194649, “Rainfall and floods in future cities”). PV has received
funding from the European Union’s Horizon 2020 research and innovation programme under the Marie Skłodowska-Curie grant agreement
310 No 101034319 and from the European Union – NextGenerationEU.



References

- Adams, C.: MAP: Where have flash flooding deaths been confirmed in Texas?, <https://www.kxan.com/news/texas/map-where-have-flash-flooding-fatalities-been-confirmed-in-texas/>, 2025.
- Ali, H., Peleg, N., and Fowler, H. J.: Global Scaling of Rainfall With Dewpoint Temperature Reveals Considerable
 315 Ocean-Land Difference, *Geophysical Research Letters*, 48, e2021GL093798, <https://doi.org/10.1029/2021GL093798>, _eprint: <https://onlinelibrary.wiley.com/doi/pdf/10.1029/2021GL093798>, 2021.
- Andria, S., Borga, M., and Marani, M.: Thermodynamic vs. Large-Scale Controls on Extreme Precipitation: Temporal Scale Dependence and Clausius-Clapeyron Scaling Redefined, *ESS Open Archive* [preprint], <https://doi.org/https://doi.org/10.22541/essoar.173655785.54054918/v2>, 2025.
- 320 Burt, S.: Cloudburst upon Hendrabortnick Down: The Boscattle storm of 16 August 2004, *Weather*, 60, 219–227, <https://doi.org/10.1256/wea.26.05>, _eprint: <https://rmets.onlinelibrary.wiley.com/doi/pdf/10.1256/wea.26.05>, 2005.
- Ebers, N., Schröter, K., and Müller-Thomy, H.: Estimation of future rainfall extreme values by temperature-dependent disaggregation of climate model data, *Natural Hazards and Earth System Sciences*, 24, 2025–2043, <https://doi.org/10.5194/nhess-24-2025-2024>, publisher: Copernicus GmbH, 2024.
- 325 Faranda, D., Ginesta, M., and Alberti, T.: Heavy rain in July 2025 Texas floods locally intensified by human-driven climate change, *Tech. rep.*, ClimaMeter, Institut Pierre Simon Laplace, CNRS, <https://doi.org/10.5281/zenodo.15829357>, 2025.
- Fowler, H. J., Lenderink, G., Prein, A. F., Westra, S., Allan, R. P., Ban, N., Barbero, R., Berg, P., Blenkinsop, S., Do, H. X., Guerreiro, S., Haerter, J. O., Kendon, E. J., Lewis, E., Schaer, C., Sharma, A., Villarini, G., Wasko, C., and Zhang, X.: Anthropogenic intensification of short-duration rainfall extremes, *Nature Reviews Earth & Environment*, 2, 107–122, <https://doi.org/10.1038/s43017-020-00128-6>, 2021.
- 330 Guerreiro, S. B., Blenkinsop, S., Lewis, E., Pritchard, D., Green, A., and Fowler, H. J.: Unravelling the complex interplay between daily and sub-daily rainfall extremes in different climates, *Weather and Climate Extremes*, 46, 100735, <https://doi.org/10.1016/j.wace.2024.100735>, 2024.
- Hardwick Jones, R., Westra, S., and Sharma, A.: Observed relationships between extreme sub-daily precipitation, surface temperature, and relative humidity, *Geophysical Research Letters*, 37, <https://doi.org/10.1029/2010GL045081>, _eprint: <https://onlinelibrary.wiley.com/doi/pdf/10.1029/2010GL045081>, 2010.
- 335 Held, I. M. and Soden, B. J.: Robust Responses of the Hydrological Cycle to Global Warming, <https://doi.org/10.1175/JCLI3990.1>, section: *Journal of Climate*, 2006.
- Kawase, H., Imada, Y., Tsuguti, H., Nakaegawa, T., Seino, N., Murata, A., and Takayabu, I.: The Heavy Rain Event of July 2018 in Japan Enhanced by Historical Warming, <https://doi.org/10.1175/BAMS-D-19-0173.1>, section: *Bulletin of the American Meteorological Society*,
 340 2020.
- Laux, P., Feldmann, D., Marra, F., Feldmann, H., Kunstmann, H., Trachte, K., and Peleg, N.: Future precipitation extremes and urban flood risk assessment using a non-stationary and convection-permitting climate-hydrodynamic modeling framework, *Journal of Hydrology*, 661, 133607, <https://doi.org/10.1016/j.jhydrol.2025.133607>, 2025.
- Lenderink, G. and van Meijgaard, E.: Increase in hourly precipitation extremes beyond expectations from temperature changes, *Nature Geoscience*, 1, 511–514, <https://doi.org/10.1038/ngeo262>, publisher: Nature Publishing Group, 2008.
- 345 Lewis, E., Fowler, H., Alexander, L., Dunn, R., McClean, F., Barbero, R., Guerreiro, S., Li, X.-F., and Blenkinsop, S.: GSDR: A Global Sub-Daily Rainfall Dataset, <https://doi.org/10.1175/JCLI-D-18-0143.1>, section: *Journal of Climate*, 2019.



- Marra, F. and Peleg, N.: TEMperature-dependent Non-Asymptotic statistical model for eXtreme return levels (TENAX), <https://doi.org/10.5281/zenodo.15291014>, 2025.
- 350 Marra, F., Borga, M., and Morin, E.: A Unified Framework for Extreme Subdaily Precipitation Frequency Analyses Based on Ordinary Events, *Geophysical Research Letters*, 47, e2020GL090209, <https://doi.org/10.1029/2020GL090209>, _eprint: <https://onlinelibrary.wiley.com/doi/pdf/10.1029/2020GL090209>, 2020.
- Marra, F., Koukoulou, M., Canale, A., and Peleg, N.: Predicting extreme sub-hourly precipitation intensification based on temperature shifts, *Hydrology and Earth System Sciences*, 28, 375–389, <https://doi.org/10.5194/hess-28-375-2024>, publisher: Copernicus GmbH, 2024.
- 355 Mistry, M. N., Schneider, R., Masselot, P., Royé, D., Armstrong, B., Kysely, J., Orru, H., Sera, F., Tong, S., Lavigne, E., Urban, A., Madureira, J., García-León, D., Ibarreta, D., Ciscar, J.-C., Feyen, L., de Schrijver, E., de Sousa Zanotti Stagliorio Coelho, M., Pascal, M., Tobias, A., Guo, Y., Vicedo-Cabrera, A. M., and Gasparrini, A.: Comparison of weather station and climate reanalysis data for modelling temperature-related mortality, *Scientific Reports*, 12, 5178, <https://doi.org/10.1038/s41598-022-09049-4>, publisher: Nature Publishing Group, 2022.
- Muñoz-Sabater, J., Dutra, E., Agustí-Panareda, A., Albergel, C., Arduini, G., Balsamo, G., Boussetta, S., Choulga, M., Harrigan, S., Hers-
 360 bach, H., Martens, B., Miralles, D. G., Piles, M., Rodríguez-Fernández, N. J., Zsoter, E., Buontempo, C., and Thépaut, J.-N.: ERA5-Land: a state-of-the-art global reanalysis dataset for land applications, *Earth System Science Data*, 13, 4349–4383, <https://doi.org/10.5194/essd-13-4349-2021>, publisher: Copernicus GmbH, 2021.
- Office, K. M.: Kumamoto Prefecture, Digital Archives of Kumamoto Disasters. Reiwa 2-nen 7-gatsu gō ni tsuite [About July 2020 heavy rainfall], <https://www.kumamoto-archive.jp/about-rain>, 2021.
- 365 O’Gorman, P. A.: Precipitation Extremes Under Climate Change, *Current Climate Change Reports*, 1, 49–59, <https://doi.org/10.1007/s40641-015-0009-3>, 2015.
- Pall, P., Aina, T., Stone, D. A., Stott, P. A., Nozawa, T., Hilberts, A. G. J., Lohmann, D., and Allen, M. R.: Anthropogenic greenhouse gas contribution to flood risk in England and Wales in autumn 2000, *Nature*, 470, 382–385, <https://doi.org/10.1038/nature09762>, publisher: Nature Publishing Group, 2011.
- 370 Peleg, N., Wright, D. B., Fowler, H. J., Leitão, J. P., Sharma, A., and Marra, F.: A simple and robust approach for adapting design storms to assess climate-induced changes in flash flood hazard, *Advances in Water Resources*, 193, 104823, <https://doi.org/10.1016/j.advwatres.2024.104823>, 2024.
- Peleg, N., Koukoulou, M., and Marra, F.: A 2°C warming can double the frequency of extreme summer downpours in the Alps, *npj Climate and Atmospheric Science*, 8, 1–9, <https://doi.org/10.1038/s41612-025-01081-1>, publisher: Nature Publishing Group, 2025.
- 375 Pfahl, S., O’Gorman, P. A., and Fischer, E. M.: Understanding the regional pattern of projected future changes in extreme precipitation, *Nature Climate Change*, 7, 423–427, <https://doi.org/10.1038/nclimate3287>, publisher: Nature Publishing Group, 2017.
- Sheridan, S. C., Lee, C. C., and Smith, E. T.: A Comparison Between Station Observations and Reanalysis Data in the Identification of Extreme Temperature Events, *Geophysical Research Letters*, 47, e2020GL088120, <https://doi.org/10.1029/2020GL088120>, _eprint: <https://onlinelibrary.wiley.com/doi/pdf/10.1029/2020GL088120>, 2020.
- 380 Trenberth, K. E., Dai, A., Rasmussen, R. M., and Parsons, D. B.: The Changing Character of Precipitation, *Bulletin of the American Meteorological Society*, 84, 1205–1218, <https://doi.org/10.1175/BAMS-84-9-1205>, 2003.
- Vohnicky, P., Hoch, J., and Thomas, E.: pyTENAX, <https://github.com/PetrVey/pyTENAX>, original-date: 2024-10-23T11:56:57Z, 2025.
- Wilson, P. S. and Toumi, R.: A fundamental probability distribution for heavy rainfall, *Geophysical Research Letters*, 32, <https://doi.org/10.1029/2005GL022465>, _eprint: <https://onlinelibrary.wiley.com/doi/pdf/10.1029/2005GL022465>, 2005.